# Numerical investigation of oil injection in a Roots blower operated as expander

IOP Conf. Series: Materials Science and Engineering **604** (2019) 012075 doi:10.1088/1757-899X/604/1/012075

# Numerical investigation of oil injection in a Roots blower operated as expander

**Nicola Casari, Ettore Fadiga, Michele Pinelli, Alessio Suman**
University of Ferrara, via Saragat 1, 44122 Ferrara, Italy

**Ahmed Kovacevic**
City, University of London, Northampton Square, EC1V 0HB, London, UK

**Sham Rane**
Department of Engineering Science, University of Oxford, Osney Mead Industrial Estate, OX2 OES, Oxford, UK

**Davide Ziviani**
Ray W. Herrick Laboratories, Purdue University, 177 S Russell Street, West Lafayette, IN, 47907-2099, USA

E-mail: nicola.casari@unife.it

**Abstract.** The adoption of positive displacement machines as expanders in Organic Rankine Cycles (ORCs) is increasingly common, especially in the low to medium power range. At the same time, these devices often serve as compressor in Vapor-Compression Refrigeration Systems. In both cases, the application of Computation Fluid Dynamics (CFD) to optimize such machines has become an integrated tool in the design process. As a consequence,several challenges associated with the numerical simulation have to be taken into account. For example, the modeling of the gap represents a challenge for the stability of the numerical analysis. The dynamic of the process, combined with deformations of the clearances and of the working chamber has to be considered with extra care.

To raise the efficiency of the machine, oil is typically injected. Its numerical modeling imply an extra challenge in the simulation of the actual operation of the machine. The present work is mainly focused on the multi-phase nature of the flow, with a particular analysis of the lubricant oil injected. In this work, a two-lobe Roots blower operated as expander has been simulated with the open-source software OpenFOAM-v1812, using the SCORG-V5.2.2. This analysis highlights the areas that are affected the most by the oil presence in order to highlight the sealing effect it provides

## 1. Introduction

ORCs have been increasingly employed in order to tackle the raise in the demand of energy combined with a cleaner way of its production. Indeed, such cycles are typically employed for waste heat recovery [1], recovering a share of energy that is typically not exploited. The component that has received attention the most by the researchers is the expander, since its

efficiency is often the most detrimental of the entire cycle [2]. This remark is more correct as the size of the plant decreases. Indeed, for plants having an output power smaller than 100 $kW_e$ (micro-ORCs), the feeding pump and the expander are the devices that are more studied.

The machines that are typically installed in micro-ORCs as pump and expander belongs to the Positive Displacement (PD) class. Several types of PD machines have been considered for these purposes, and an example of comparative analysis can be found in [3] for refrigeration and both [4] and [5] report a brief overview of the most used type of expanders in ORCs. Among the others, the Roots technology has found a number of applications in ORCs. For example, it is widely used for the heat recovery in long haul truck [6], as expander in stationary plants [7] or even for fuel cell applications [8]. This machine is particularly applied for its cost effective, reliable, and efficient operation.

A fashion to increase the efficiency of the machine is the oil injection inside the working chambers. The oil acts as a sealant agent between the various parts of the device, closing leakages paths, lubricating, cooling the machine. It is then necessary to study how device working conditions are affected by the presence of such a sealant, in terms of efficiency thickness of the oil film and zones in which fluid can stagnate or affect the normal behaviour of the expander. Indeed, studies on PD machines in general have found that oil injection ports position strongly affects the efficiency of the machine, in term of filling factors and power [9]. Other researchers, e.g. Ziviani et *al.* [10], when studying a micro-ORC whose expander has been adapted from a single-screw compressor, observed that by halving leakages and friction losses, isentropic efficiency could reach values of above 70 %: to reduce friction and leakages, one way is to increase the amount of oil circulating in the expander.

The diffusion of Roots machines has pushed researchers to look into such devices, in order to improve their efficiency. A useful tool for the prediction of flow behaviour and performance is the Computational Fluid Dynamics (CFD) analysis, for example [11]. The experimental campaign may be very challenging, due to the geometrical complexity and the compatibility of the instrumentation. Therefore, the numerical approach may be a helpful way to investigate the potential behaviour of the machine with new fluids without major changes to be carried out. Nonetheless, the complexity of the simulation has brought about the birth and the application of several numerical techniques. A brief yet comprehensive review of the possible methods for the simulation of PD machines that are usually available with common software is reported in [12]. Among the several issues that derives from the numerical approach applied to these machines, the high mesh deformation asks for extra care during the mesh generation and motion evolution phases.

To tackle the mesh motion problem, different approaches have been developed over the years. The method implemented into the SCORG software and used in this work makes advantage of the employment of body-fitted structured grids. Such meshes are easily stretched without losing quality, allowing for simulating the PD machine operation without need for remeshing, if the motion is properly solved. This approach is particularly appreciated since the alignment between wall and edge in the nearby of the wall is always respected and resolution of the flow close to the boundary is generally well resolved. The "Custom Predefined Mesh Generation Algorithm" is used in this work [13] and the technique adopted is explained in [14, 15, 16].

In order to solve the flow field, including the presence of the oil inside the machine, the open-source OpenFOAM-v1812 software has been used. The droplets are individually tracked in a Eulerian-Lagrangian approach, to better predict the trajectory of each particle and evaluate the impact areas. This work is proposed to prove the capabilities of the implementation of the mesh moving technique by the authors [11, 17] when the machine operates as expander instead of compressor. Besides, the particle tracking algorithm has been coupled with the dynamic motion solver inside the CFD, with the aim of represent always more accurately the actual operation of these machines.

## 2. Methodology

### *2.1. Geometry*

The machine investigated in this work is a two lobes Roots blower, whose operation has been reverted for working as expander. The overall geometry of the lobes, of the casing and of the working chamber area of the machine is reported in Fig. 1. The volume sealed by each of the lobe is roughly 0.00019 $m^3$.

A crucial role in the performance of PD machines is played by the size of the gap, that should be lowered as much as possible to have the lowest leakages [18]. The machine that has been investigated here has a gap that is noticeably high with respect to the common engineering practice. Specifically, the maximum clearance verifies at the interlobe passage and is around 400 $\mu$m. Even the gap between rotor and casing is quite high, being around 200 $\mu$m.

### *2.2. Mesh Generation*

In this paper, the deforming grid of the twin screw machine is generated using algebraic transfinite interpolation treated as an initial mesh upon which Elliptic Partial Differential Equation (PDE) of the Poissons form is solved [19]. The resulting differential grid has highly improved cell quality and distribution. The rotor mesh must be coupled with the suction and the discharge ports. The mesh of such ports, has been generated with the open-source software cfMesh [20]: a cartesian cut-cell grid has been generated. The rotating domain is divided from the port static one by means of ACMI (Arbitrary Coupling Mesh Interface). Since the rotor axial patches do not completely overlap the ports, the interface has to automatically detect whether fluxes must be exchanged (when fluid-fluid cells are exposed) or not (e.g. when the interface is between fluid and solid cell). Specifically, the Casing-To-Rotor, non conformal approach is used. In such framework, an non-conformal interface is placed among the two lobe regions.

Once the mesh is generated, it must be exported to OpenFOAM readable format. This feature is not yet available into SCORG. For the current analysis, the mesh translation was done via ANSYS-CFX and ICEM. The direct exportation of the mesh is considered a next step in this research.

In order to correctly replicate the operation of the machine, the rotors motion must be considered. Such rotation causes the deformation of the computational domain and thus the mesh should accomodate such displacement. The strategy adopted in this work is to generate a structured computational mesh for an initial position, as reported in the section 2.2. At this point a user-defined number of grids per rotor pitch is generated and written in separate files. Each of the file contains the control points (coordinates) through which the computational nodes has to pass during the machine operation. This entire procedure is carried out within the SCORG-v5.2.2 framework. In the current work, a set of 180 files per groove are generated, meaning there are 180 points through which a moving mesh node has to pass to cover a pitch. This translates in a mesh per degree of rotation.

The dynamic motion solver implemented in the CFD software therefore updates the mesh position for each of the time step, having the grid files as a reference. To calculate the position of a node for the $i-th$ time step, equation 1 is solved

$$x_{i,final} = \alpha x_{i,AG} + (1-\alpha)\, x_{i,NG} \tag{1}$$

where the subscript AG represents the actual grid file and NG is for the next grid file. AG and NG are the files written by SCORG containing the node postion at the two time instant the solver is interpolating among. $x_i$ represents the position of the node at the corresponding grid file (when the subscript AG or NG is reported). The parameter $\alpha$ is the blending factor among the two time instants. This algorithm has been added to the mesh motion libraries available in OpenFOAM-v1812.

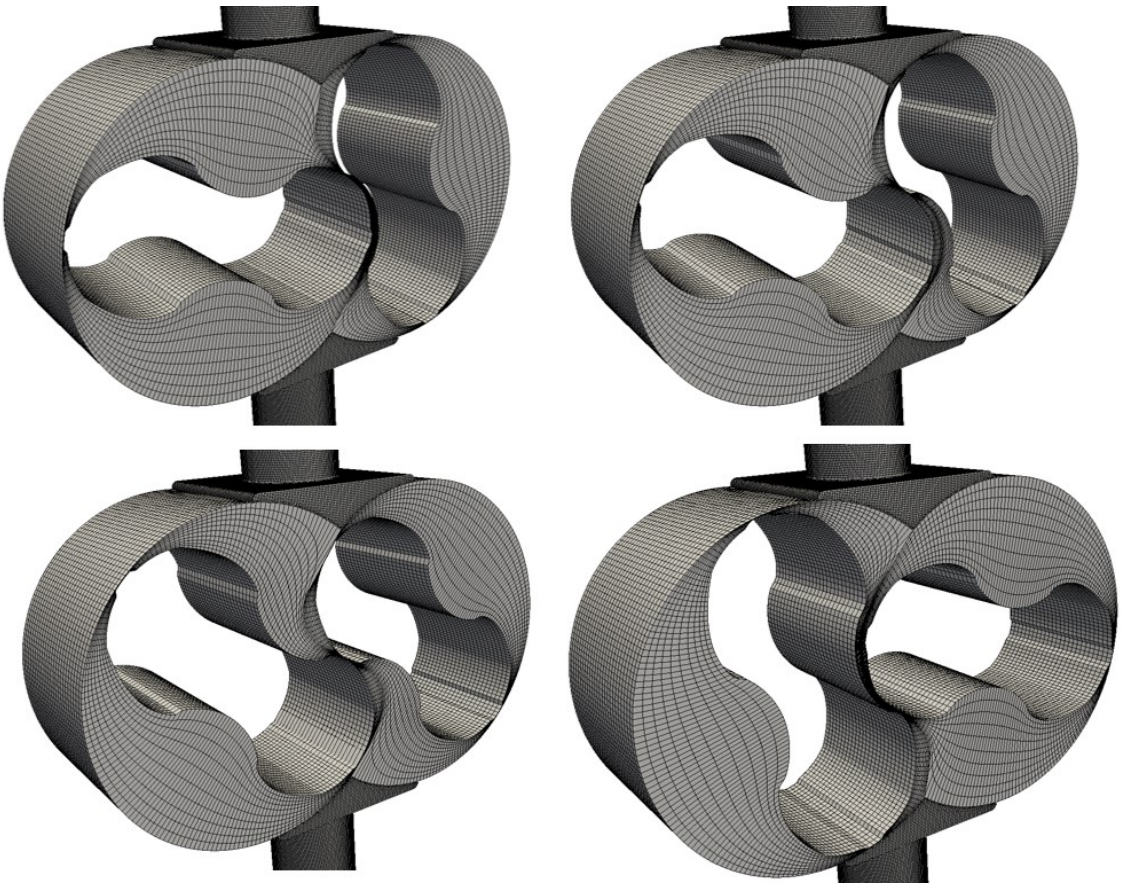

**Figure 1.** Computational mesh realized on the rotors, as imported in OpenFOAM. Evolution of the mesh displacement: from left to right, from up to bottom it is clear the high level of stretching of the mesh.

The linear interpolation proposed in Eq. 1 is tremendously important in the persent analysis. Indeed, particle tracking in a lagrangian approach requires the condition CFL $< 1$ (Courant-Friedrichs-Lewy) to be strictly respected [21]. This is true for either explicit or implicit solvers since it is related to the computation of the particle trajectories: guarantees that each particle crosses at most one cell boundary at every time step. This condition is required for having an accurate prediction of the particle impact location. Therefore, it becomes compulsory to decouple the time step from the grid files obtained by SCORG.

*2.3. Numerical Analysis*

The case was simulated under the boundary conditions reported in Table 1. The turbulence has been included by means of the SST k-$\omega$ turbulence model.

The algorithm proposed in this work is implemented in such a fashion to be consistent with the classical OpenFOAM management of the inputs. Particularly, the inputs required in the *dynamicMeshDict* for using the SCORG framework are reduced as much as possible. Specifically, the user is required to generate three different pointzones in the case of the non-conformal approach. Indeed one zone is for the female lobe, one for the male lobe (this two regions are not required in the case of conformal mesh, and just the rotor part is required, being the rotor zone a single domain), and the stationary points. The other inputs are the number of grids per pitch and the number of grooves. These inputs are necessary for simulating the operation of the

**Table 1.** Boundary conditions for the computation of the flow field. he pressure difference has been considered in order to be consistent with the original compressor operation.

| | Quantity | Value |
|---|---|---|
| Inlet | $p_0$ | 116,000 Pa |
| | $T_0$ | 293 K |
| | Turbulence intensity | 1 % |
| | Turbulence mixing length | 0.0021 m |
| Fixed Walls | T | adiabatic |
| Rotating Walls | $\omega_{male}$ | 1500 rpm |
| | T | adiabatic |
| Outlet | p | 101,000 Pa |

machine for multiple revolutions. Lastly the rotational speed in rad/s has to be provided.

The oil injected has been treated from a lagrangian standpoint. The configuration tested in this work is depicted in Fig. 2. Specifically, the nozzle has been placed just before the working chambers, and on symmetrically with respect to it. This layout is thought to be more effective with respect to the premixed configuration, as reported in [22], and is therefore investigated. Throughout the present analysis, the fluid investigated is air considered as ideal gas. It must be remarked that, in the actual working condition, this machine should operate R245fa. Therefore, the choice of the properties of the oil must consider the compatibility issue with such gas. In light of this track, the properties of the oil are taken from [23].

The particle size distribution injected by the nozzle has been imposed by considering the remarks of [24] and [25]. From their analyses, it has become clear that oil droplets can reach the size of 1 mm, even if the most effective droplet diameter has found to be around 100 $\mu$m. Given this, in the present work, the particle size distribution injected follows the Rosin-Rammler law, as suggested in [26]. The distribution parameter required by the software are the mean diameter d = 150 $\mu$m and the dispersion coefficient n = 0.5. The thermophysical properties of the oil relevant to the particle tracking (incuding the heat transfer) are the density $\rho = 959$ kg/m$^3$ and the specific heat $c_p = 2800$ kJ/(kg K). These properties are assigned to each of the droplet that is sampled from the size distribution assigned. The injection velocity is considered to be equal to 50 m/s.

The lagrangian particle tracking is computed by solving a force balance on the particle. Due to the particle size, the only force kept into account in this work is the drag force, and its implementation in OpenFOAM is reported in [27].

A last remark regards the behaviour of the particle upon impact against the rotors or the wall. Particles could stick or rebound upon impact, depending on its kinematic properties and on the conditions of the substrate. If sticking happens, the droplet contributes in forming a liquid film on the wall, that act as a sealant. In this work, each impact is considered to entail sticking, but the film growth is not considered. The present analysis focuses only on the impact locations, and the growth of the film in the rotating area is considered a next step in this track.

The solver employed in this work is a modification of *sonicDyMFoam*, which belongs to the compressible set of solver that comes with the software OpenFOAM-v1606+. This solver employs PISO algorightm [28] with inner integration performed with SIMPLE strategy [29]. The implementation in the OpenFOAM framework is described in [30]. This solver can automatically take into account any mesh motion input given by the user. In this work, the developed algorithm is enclosed in a library read by the *dynamicMeshDict*, that is the dictionary that asks for any mesh motion input. The library is dynamically linked during the compilation. The simulations run fully parallel thanks to the open MPI library. Extra-care should be taken when decomposing

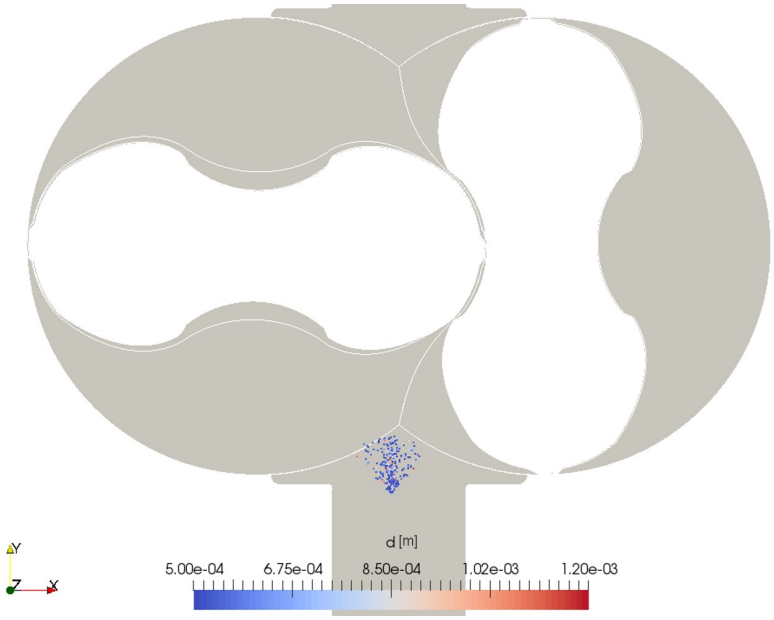


**Figure 2.** Position of the injector and shape of the spray. The color bar shows the particle size distribution, in meters.

the domain, due to the presence of non-conformal interfaces at the inlet and outlet ports. To enforce mass conservation, both the sides of the ACMI interface are forced to stay on the same processor. This feature comes with the standard installation of OpenFOAM.

The modification to the standard solver has been introduced for adding the support for the lagrangian phase. The standard installation of OpenFOAM provides only the lagrangian solver *sprayDyMFoam* for considering both the moving mesh and the active coupling between particles and flow field. Active means that two-way coupling is performed[31]: the flow field affects the particle motion and vice-versa. In cases in which particles have high concentration or high inertia, the effect of the influence they have on the carrier phase is not negligible. This remark translates in dispersed phase being a sink both in terms of momentum and energy. The need for the new solver is related to the fact that *sprayDyMFoam* is mainly employed for combustion analyses. Therefore, an accurate evaluation of the reactions and of the chemical components of both oil and carrier phase should have been considered. Furthermore, the simulation with such an approach is unstable and likely to blow up after few time steps.

The new solver has been named *sonicParcelDyMFoam* to be consistent with the OpenFOAM's fashion of naming solvers. The thermodynamics of the carrier phase has been included considering air as ideal gas, having constant thermophysical properties.

## 3. Results

The full-3D CFD analysis of the expander under the boundary conditions reported in 1 is reported here. It must be remarked that the axial gaps are not included in this study.

### *3.1. Flow field analysis*

The analysis will firstly focus on the overall performance of the machine without the presence of oil, that will be described in the section 3.2.

Considering the pressure evolution, figure 3 reports the pattern just before the closure of the working chamber by the right hand side lobe. It can be seen that the gaps, even if quite big, are sufficiently small not to disrupt the pressure distribution: the pressure drop across the

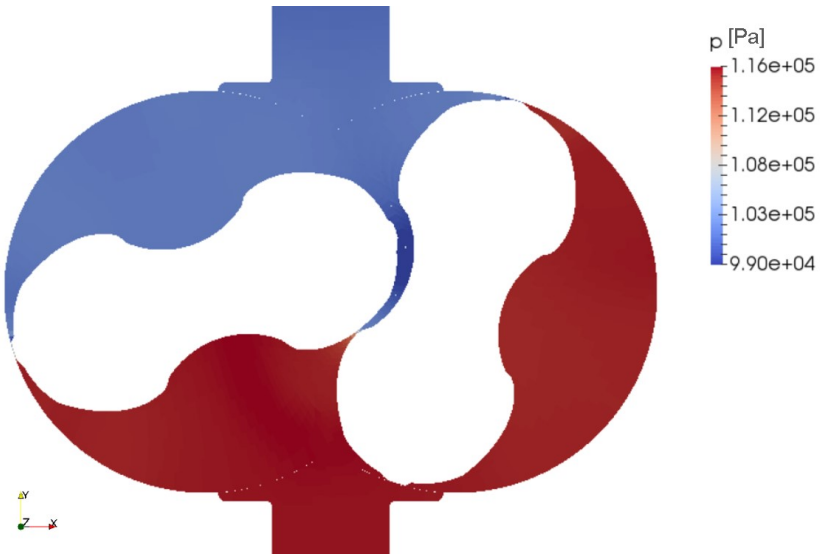


**Figure 3.** Pressure distribution at the closing of the suction port for the right hand side lobe

gap is equal to the overall pressure ratio of the machine. The lowest pressure recorded, in this configuration, is downstream the interlobe gap. This underpressure is related to the high speed of the flow that arise in this area (around 100 m/s).

The parameter considered for the evaluation of the performance of the Roots-type expander is the torque. The variation of such parameter over half of the revolution of the rotors is reported in Fig. 4. Such interval is representative of the entire operation of the machine, considering the fact that the rotors are perfectly symmetrical. It can be seen that the variation of the torque is quite big, with a maximum slightly smaller than 1 Nm up to a minimum where almost no useful work is extracted from the flow. This happens when the lobe position is such that the sealing is complete and the working fluid is entirely comprised within the working chamber, without exchanging mass with the suction or the supply. Considering only the LHS rotor (blue line), it can be seen that the torque value it records is basically constant around 0.6 Nm over the first 60 degrees of rotation. This time slot corresponds to the filling period of the chamber. Around 60°, the moment that can be extracted from this rotor reaching it peak around 70°. In this range, the chamber is completely closed (except the gaps) and therefore the maximum work can be extracted. After such point, the torque lowers as a consequence of the opening towards the discharge port. A peak arise after 80° of observation window: the working chamber is, at this point, at the discharge pressure value as is the upper part of the lobe (that shows high velocity areas downstream the interlobe gap lowering even more the static pressure). At the same time the lower part of the LHS rotor is exposed to the high pressure of the suction port. Therefore a second peak arises, though with a lower intensity with respect to the first one. From this point onward, the useful work that can be extracted from the machine keeps on lowering until the very minimum, that occurs when the rotor becomes horizontal (main axis of the lobe perpendicular to the suction-discharge axis).

In the same graph, the power that is extracted from both the lobes is reported. The variation of the power can be as high as 125 W, having an average of roughly 175 W. The ripple in the output confirms the major drawback of the two-lobes machines, that is having high pulsations in the flow rate and in all the related quantities.

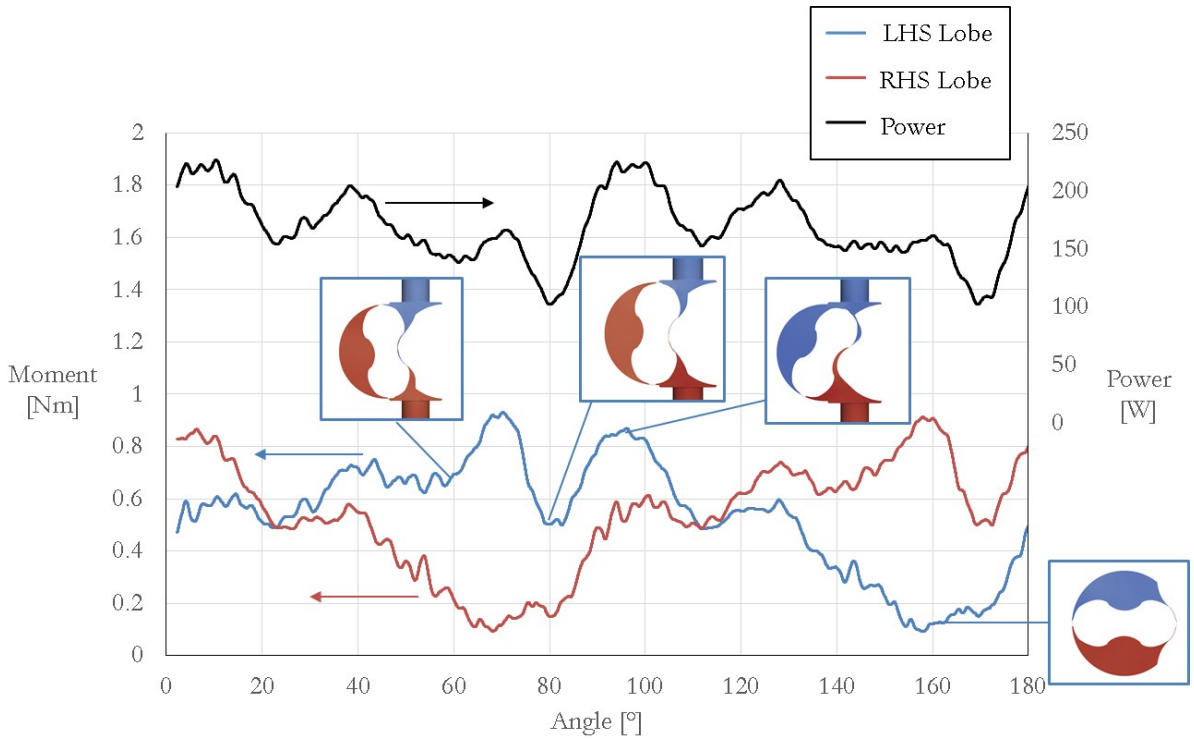


**Figure 4.** Torque evolution on the Left Hand Side (LHS) and Right Hand Side (RHS) lobes recorded for half of the revolution. The contours represent the pressure values.

### *3.2. Oil Injection*

The oil injection should affect the performance of the machine in terms of gap reduction and by affecting the expansion and making it more similar to an isothermal transformation. The blockage of the gap as a consequence of the particles injected can be accounted for only by considering the growth of the liquid film on the walls. This phenomenon has not been included in the current work: the software capabilities of modelling this feature currently do not support the moving mesh.

For what concerns the temperature reduction, the effect of the oil presence on the gas is marginal. Indeed, the temperature of the oil is basically constant. Such negligible effect is related to the small temperature decrease of the fluid going through the machine. Such effect would be much larger in compressors or expanders having an higher pressure ratio.

It is however of interest to investigate the area in which the droplets impact. With the configuration tested, both the rotors are wet with an high flow rate of oil. The droplets impinging rate is higher in the mid of the width and very low at the axial ends of the rotors. This is qualitatively reported in fig. 5a. From the same figure it is clear that the casing does not record any impacts. No sticking event is indeed recorded over the observation period. Some of the oil, with the configuration tested, hits on the axial walls. Thanks to such contribution, the performances of the machine should be improved if the axial gaps are considered as well.

A last remark regards the penetration distance of the droplets, $d_p$, meaning the distance the droplets can travel before impinging on a surface. This quantity is analyzed in fig. 5b, showing that the maximum penetration distance occurs in the interlobe area. During the revolution, the droplets are never able to make their way beyond half of the lobe height. Considering the working chambers in the sealing phase, no oil is found in these areas, showing a bad configuration if the aim is to maintain constant the gas temperature for increasing the expansion efficiency.

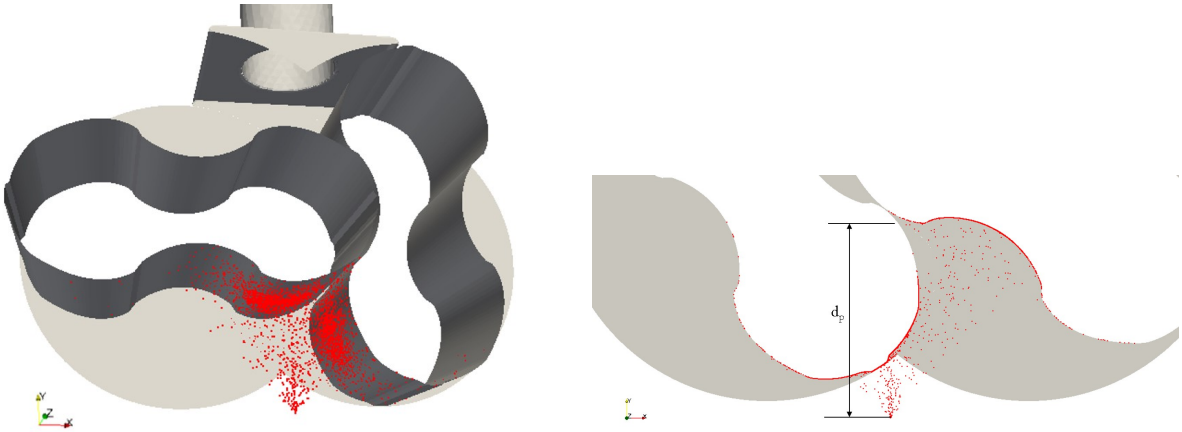


**(a)** Impinging areas of the oil droplets

**(b)** Penetration distance and particular of droplets distribution in the interlobe gap

**Figure 5.** Oil injection details

From these considerations, a different position for the nozzle should be considered. Specifically, the oil should be injected upwind, in order to be able to mix it with the gas in the working chamber.

## 4. Conclusion

In the current study, the mesh motion libraries that link the pre-defined set of files containing the control points for the mesh motion (provided by SCORG) and the flow solver (OpenFOAM-v1812) have been refined and updated. The user-required inputs for the mesh motion routine have been reduced, making the new routine compliant with the standards of openfoam for dynamic mesh libraries. Additionaly, the support for the lagrangian phase has been added, in order to include the oil injection to the numerical investigations that can be carried out with such open-source tool.

Here, the procedure has been applied to a Roots blower. Specifically, its operation has been reverted and the machine works as an expander. The flow field analysis inside the machine has shown the source of the ripple in the torque. This behaviour is characteristic of this type of machine, and it is among the reasons that drive the choice of expander towards higher lobe numbers.

Although the machine considered has gaps that are quite large if compared to common engineering practice, the performance of a realistic device has been analysed with particular care to the oil injection. The placing of the injector right before the meshing area has shown a good impingement pattern on the rotors.

The implementation proposed in this work shows good robustness and flexibility, expanding the OpenFOAM capabilities in modeling PD machines. Future work in this track will be devoted to include the accretion of the liquid film on the walls, and the interaction of such thin layer with the flow field.

## 5. Acknowledgement

The research was partially supported by the Italian Ministry of Economic Development within the framework of the Program Agreement MSE-CNR "Micro co/tri generazione di Bioenergia Efficiente e Stabile (Mi-Best)".

## References

[1] Hung T C, Shai T and Wang S K 1997 *Energy* **22** 661–667
[2] Bianchi M, Branchini L, Casari N, De Pascale A, Melino F, Ottaviano S, Pinelli M, Spina P and Suman A 2019 *Applied Thermal Engineering* **148** 1278–1291
[3] Tassou S and Qureshi T 1998 *International Journal of Refrigeration* **21** 29–41
[4] Ziviani D, Gusev S, Lecompte S, Groll E, Braun J, Horton W T, van den Broek M and De Paepe M 2016 *Applied Energy* **181** 155–170
[5] Quoilin S, Declaye S, Tchanche B F and Lemort V 2011 *Applied thermal engineering* **31** 2885–2893
[6] Subramanian S 2015 Heavy duty roots expander heat energy recovery (hd-reher) Tech. rep. Eaton Corporation, Menomonee Falls, WI (United States)
[7] Orlandini V 2017 *Waste heat recovery systems: numerical and experimental analysis of organic Rankine cycle solutions* Ph.D. thesis alma
[8] Stretch D, Wright B, Fortini M, Fink N, Ramadan B and Eybergen W 2016 Roots air management system with integrated expander Tech. rep. Eaton Corporation, Menomonee Falls, WI (United States)
[9] Stošic N, Milutinović L, Hanjalić K and Kovačević A 1992 *International Journal of Refrigeration* **15** 206–220
[10] Ziviani D, Gusev S, Lecompte S, Groll E, Braun J, Horton W, van den Broek M and De Paepe M 2017 *Applied energy* **189** 416–432
[11] Casari N, Pinelli M, Suman A, Kovacevic A, Rane S and Ziviani D 2018 *IOP Conference Series: Materials Science and Engineering*
[12] Casari N, Suman A, Ziviani D, van den Broek M, De Paepe M and Pinelli M 2017 *Energy Procedia* **129** 411–418
[13] Rane S 2015 *Grid generation and CFD analysis of variable geometry screw machines* Ph.D. thesis City University London
[14] Kovacevic A, Stosic N and Smith I 2007 *Screw Compressors: Three Dimensional Computational Fluid Dynamics and Solid Fluid Interaction* vol 46 (Springer Science & Business Media)
[15] Rane S and Kovacevic A 2017 *Advances in Engineering software* **107** 38–50
[16] Kovacevic A and Rane S 2017 *Advances in Engineering Software* **109** 31–43
[17] Casari N, Pinelli M, Suman A, Kovacevic A, Rane S and Ziviani D 2018 *IOP Conference Series: Materials Science and Engineering* vol 425 (IOP Publishing) p 012017
[18] Casari N, Suman A, Morini M and Pinelli M 2017 *Energy Procedia* **129** 248–255
[19] Thompson J F, Soni B K and Weatherill N P 1998 *Handbook of grid generation* (CRC press)
[20] Juretić F 2015 *Zagreb, Croatia*
[21] Casari N, Pinelli M, Suman A, di Mare L and Montomoli F 2018 *Journal of Turbomachinery* **140** 061001
[22] Randi S, Suman A, Casari N, Pinelli M and Ziviani D 2018 *IOP Conference Series: Materials Science and Engineering* vol 425 (IOP Publishing) p 012001
[23] Zhelezny V, Semenyuk Y V, Ancherbak S, Grebenkov A and Beliayeva O 2007 *Journal of Fluorine Chemistry* **128** 1029–1038
[24] Ziviani D, Bell I H, De Paepe M and van den Broek M 2016
[25] Valenti G, Colombo L, Murgia S, Lucchini A, Sampietro A, Capoferri A and Araneo L 2013 *Applied Thermal Engineering* **51** 1055–1066
[26] Yoon S, Hewson J, DesJardin P, Glaze D, Black A and Skaggs R 2004 *International Journal of Multiphase Flow* **30** 1369–1388
[27] López A, Nicholls W, Stickland M T and Dempster W M 2015 *Computer Physics Communications* **197** 88–95
[28] Issa R I 1986 *Journal of computational physics* **62** 40–65
[29] Patankar S 1980 *Numerical heat transfer and fluid flow* (CRC press)
[30] Jasak H 1996 *Error analysis and estimation for the finite volume method with applications to fluid flows.* (Imperial College London (University of London))
[31] Elghobashi S 1994 *Applied Scientific Research* **52** 309–329